

Response of Exothermic Additions to the Flux Cored Arc Welding Electrode — Part 2

Investigating the exothermically reacting stoichiometric mixtures of aluminum, magnesium, and aluminum/magnesium (50/50 wt-%) flux additions in the flux cored arc welding process

BY S. H. MALENE, Y. D. PARK, AND D. L. OLSON

ABSTRACT. In Part 1 of this investigation, exothermically reacting magnesium-type flux additions to the flux cored arc (FCA) welding consumable electrode have resulted in measurable increases in the arc process efficiency. In Part 2 of this investigation, the manufacture and heat delivery of stoichiometric mixtures of aluminum, magnesium, and aluminum/magnesium (50/50 wt-%) flux types, with the mineral form of Fe_2O_3 termed hematite systematically displacing iron powder, were studied in an experimental self-shielded FCA flux formulation. All welds made using Part 2 electrodes were acceptable at the same preassigned welding schedule indicating an increase in usable weld parameter space. The Al/Mg (50/50 wt-%) electrodes were significantly more effective than aluminum or magnesium flux additions in net gain value. Since a reduction in the electrical power consumed, brought about for a given welding condition by the addition of chemical heating components, is as beneficial as a directly measurable increase in heat input (in joules) over the baseline condition, a composite normalized energy scale, in relative percent, is composed. By subtracting the percent electrical power (difference from the baseline value) from the percent measured heat input (also the difference from the baseline value) for each welding condition, a net gain value is calculated. The aluminum reactive addition at up to 20 wt-% was found to have a 32% increase over the baseline in specific deposit (g/kW consumed). The magnesium-reactive addition at 40 wt-% yielded a 38% increase in specific deposit and the Al/Mg (50/50 wt-%) electrode exhibited a 49% increase in specific deposit at only 10 wt-% reactive addition. Consequently, the investigation of Part 2 electrodes with the FCA welding

S. H. MALENE (stephen.malene@srnl.doe.gov) is with Savannah River National Laboratory, Aiken, S.C. Y. D. PARK is with Dong-Eui University, Dept. of Advanced Materials Engineering, Busan, Korea. D. L. OLSON is with Colorado School of Mines, Dept. of Metallurgical and Materials Engineering, Golden, Colo.

process has shown that a maximum gain value occurs between the 10 and 20 wt-% electrodes of the Al/Mg (50/50 wt-%) flux additions. Much less electrical power was used for these electrodes than was consumed in the baseline comparative.

Introduction

Field repair welding traditionally requires bulky dedicated electrical equipment or gas bottles with attendant torches, hoses, and regulators along with considerable operator skill. This type of welding can be enhanced through the use of exothermic flux additions to the FCA welding process (Refs. 1, 2). The self-shielding nature of the process precludes the need for gas systems while a reduction in electrical energy dependence of the welding parameter schedule as measured through voltage and amperage levels broadens the user appeal and applicability. Part 1 of this investigation (Ref. 3) showed that the exothermic reactions caused by the magnesium flux additions of the FCA welding consumable electrode demonstrated significant increases in the arc process efficiency. When the process efficiency was corrected for an apparent reduction in electrical power consumed in addition to the increase in measured heat input, the maximum benefit occurred at around 30 wt-% magnesium flux rather than at the 20 wt-% level for the measured heat input variable alone (uncorrected for a reduction in electrical power consumed). There was no evidence of uncontrolled reaction, which was observed in the

unconstrained exothermic chemical additions to the flux formula of the shielded metal arc (SMA) welding process (Ref. 2).

Two pure metallic elements that reduce iron oxide, aluminum and magnesium, are used in the production of steel to deoxidize or kill the steel. These elements have been added to the flux in various flux-related arc welding processes to kill the weld pool, and the reactions are exothermic. In addition, these elements, in large enough quantities, are known to be able to provide significant heat for welding (Ref. 4). Karpenko (Ref. 5) reported the effects of exothermic additions (aluminum + iron oxide) on the melting characteristics of SMA electrodes. The results show that aluminum additions increase the weld deposition rate and enhance welding parameters to achieve improved productivity. Also, Glushchenko (Ref. 6) studied the effects of exothermic additions in submerged arc welding fluxes on deposition rate and melting efficiency. Allen et al. showed that exothermic flux additions, such as aluminum and Al/Mg (50/50 wt-%) flux additions to SMA welding electrodes can assist in the generation of heat and increase the rate of electrode melting. Applying Hess's law and integrating the heat capacity from room temperature to that of the molten steel weld pool temperature gives the quantity of heat produced by the aluminum or magnesium reactions with hematite. Table 1 shows the calculated amount of heat released during the proposed reactions. These reactions are extremely violent if only the metal oxide and the pure reducing metal are used without mitigating chemical compositional control.

Part 2 of this investigation focuses on the revised (stoichiometric) exothermic flux formulations — aluminum, magnesium, and Al/Mg (50/50 wt-%) flux additions. Aluminum plus hematite, magnesium plus hematite, and a 50-50 mix of the Al/Mg types of exothermic reactions were prepared and evaluated. Also, this investigation was aimed at finding the potential effectiveness of such exothermic flux ad-

KEYWORDS

Flux Cored Arc (FCA) Welding
Aluminum
Magnesium
Electrode
Electrical Power
Heat Input
Shielded Metal Arc (SMA)
Welding

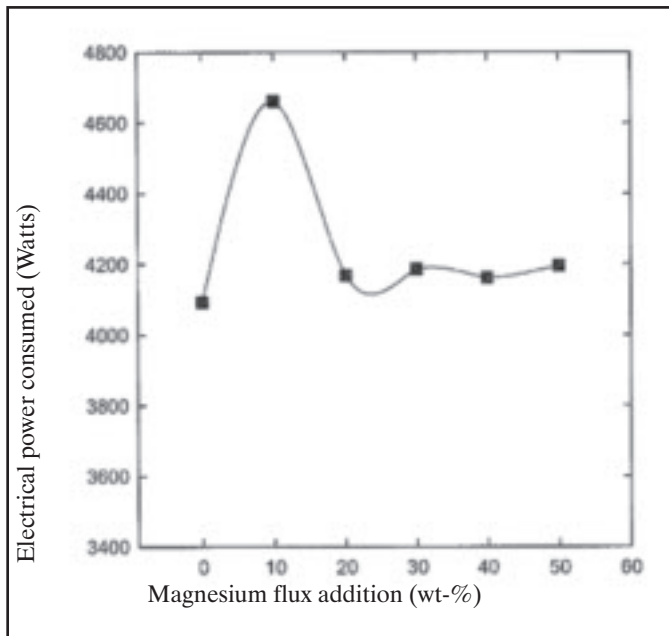
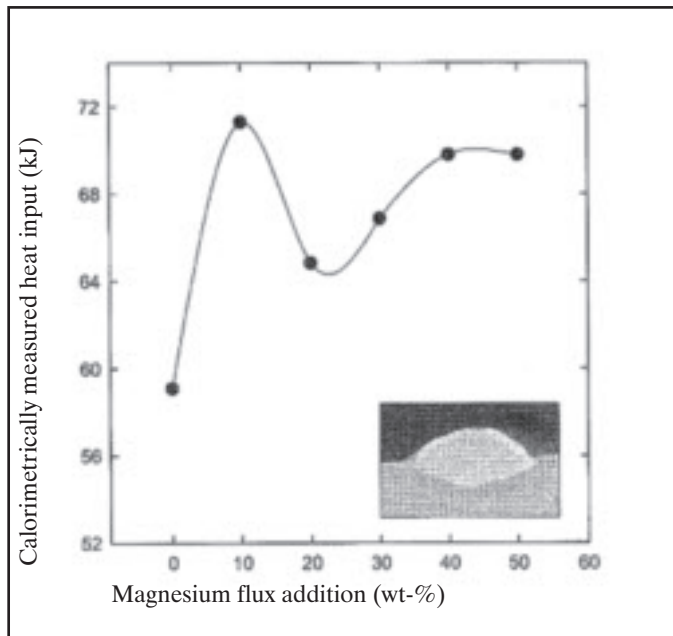


Fig. 1 — Measured heat input as a function of wt-% magnesium flux addition at 110 in./min (47 mm/s) melting rate. The insert photograph is bead morphology of weldment with 40 wt-% of magnesium flux type electrode.

Fig. 2 — Electrical power consumed as a function of wt-% magnesium flux addition at 110 in./min (47 mm/s) melting rate.

Table 1 — Enthalpy Heats of Reaction for Aluminum and Magnesium Plus Hematite Flux Additions

Addition Reaction	Enthalpy (kJ/mol O ₂)
2Al + Fe ₂ O ₃ = Al ₂ O ₃ + 2Fe	850
3Mg + Fe ₂ O ₃ = 3MgO + 2Fe	1060
Al/Mg (50/50) mix with Fe ₂ O ₃	Quantity of heat between 850 and 1060

Table 2 — Flux Composition for Part 2 Electrodes, Parts by wt-%

Flux Compound	Baseline Electrode	Aluminum-Type Electrode	Magnesium-Type Electrode	Al/Mg (50/50) Type Electrode
CaF ₂	15	15	15	15
TiO ₂	15	15	15	15
CaCO ₃	6	6	6	6
SiO ₂	4	4	4	4
Fe	60	50 ~ 10	50 ~ 10	50 ~ 10
2Al + Fe ₂ O ₃	—	10 ~ 50	—	—
3Mg + Fe ₂ O ₃	—	—	10 ~ 50	—
Al/Mg (50/50) + Fe ₂ O ₃	—	—	—	10 ~ 50

ditions to the flux cored arc welding consumable electrode, and the effect of exothermic additions on the weld deposit and the arc/electrode extension environment were studied.

Experimental Procedures

As with investigation by Allen et al. (Refs. 1, 2) of the SMA welding system, three types of exothermic reaction powders were studied: the aluminum plus hematite, the magnesium plus hematite, and a 50/50 mixture of the magnesium and aluminum plus hematite mixtures. A self-shielding flux formulation containing 60 wt-% iron powder was selected as the baseline. The iron powder was systematically displaced with stoichiometric mixtures of the exothermic metal(s) and hematite in batch ratios from 0 to 50% in steps of 10% (±1.0 %) and a fixed fill ratio of 15%. The Part 1 electrode wires were produced with 17 to 18 wt-% flux fill to

steel sheath ratios. Initial drawing difficulties led to all of these later Part 2 electrodes being manufactured to a more reasonable and commercial-like 15 wt-% fill. The set of 15 welding wires plus a new baseline electrode produced were made with stoichiometric mixtures of black, crystalline (granular) hematite (of between 100 and 140 mesh) and evaluated as to relative heat input and reduction in electrical power consumed to produce the weld.

The coarse-grained hematite was used in stoichiometric concentration levels with aluminum, magnesium, and Al/Mg (50/50 wt-%). Each of the three types of exothermic additions was added to the flux in place of the iron powder base in 10 wt-% increments up to 50 wt-%. The linear densities for all of these electrodes show much less variation than in the previous study and measure about 0.12 g/cm. The lower packing density of the flux and the change to a coarse-grained hematite allows for a

more constant linear density value as a function of exothermic concentration level. These flux compositions are presented in Table 2.

Table 3 lists the welding parameters used in this study. The actual voltages recorded were about one volt higher, on average, than the set voltage. No slope-in, slope-out, or crater fill times were used. The torch head was adjusted to vertical with respect to the baseplate samples to be welded, and the travel direction was parallel to the length of the sample and centered along the surface. The wire feed speed was held constant at 110 in./min. All data points represent an average of a minimum of at least three identical weld trials.

In addition to machine current and voltage recordings for each 20-s timed weld sample, the wire electrode was cut off even with the guide tube following the weld and was bagged, tagged, and measured for length and mass. While most electrode extension remnants did not

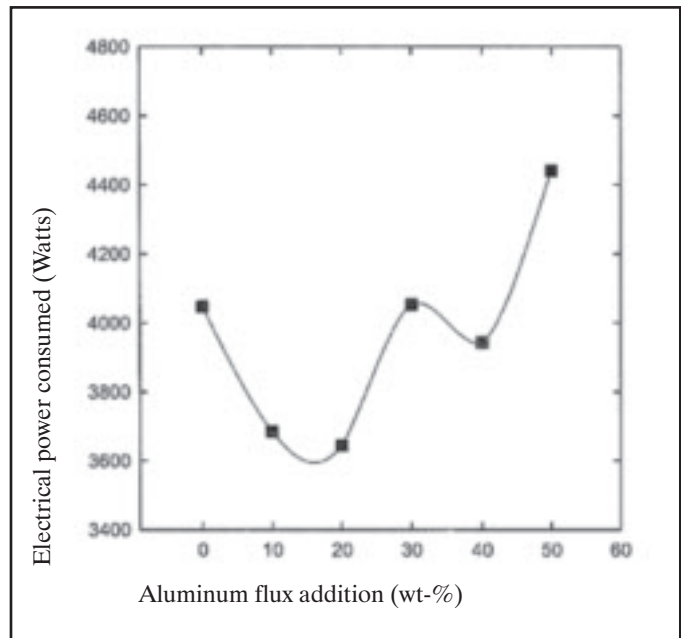
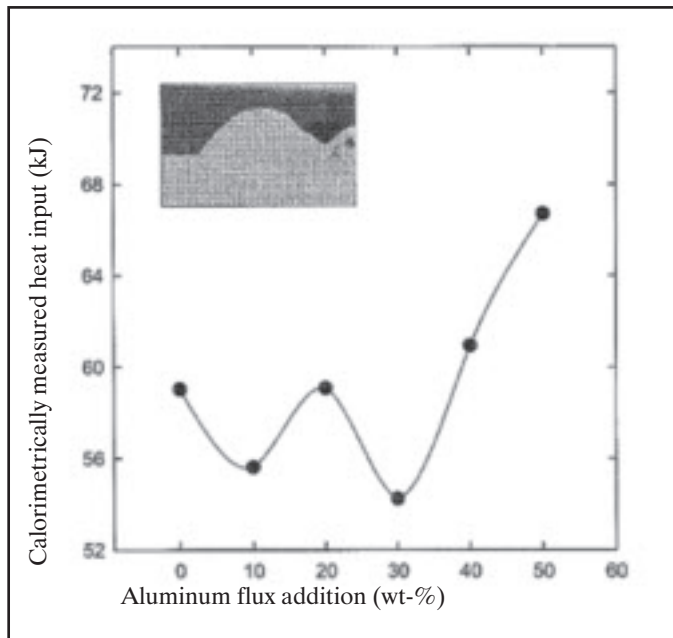


Fig. 3 — Measured heat input as a function of wt-% aluminum flux addition at 110 in./min (47 mm/s) melting rate. The insert photograph is bead morphology of weldment with 20 wt-% of aluminum flux type electrode.

Fig. 4 — Electrical power consumed as a function of wt-% aluminum flux addition at 110 in./min (47 mm/s) melting rate.

show evidence of the formation of a solidified ball on the arc end, indicative of operation within the spray transfer mode, some electrodes had what appeared to be the beginnings of a ball that may have been formed after the electrical current was shut off. The ball-like protrusions were noted but ignored in the length and mass measurements for electrode extension. While this method of shutting off the welding machine and then snipping the electrode that was left sticking out from the guide tube may not be precisely representative of the steady-state weld electrode extension, it was performed in this manner as a matter of convenience strictly for comparative purposes.

A liquid nitrogen calorimeter was used to measure the amount of heat that was transferred into the base metal when welding with exothermically assisted consumables. The detailed description of the calorimetric measurement is in Part 1.

The weld deposits were cut, ground, polished, photographed, and measured with an image analysis system. The deposited slags and weld beads were visually examined, and welding was uniform and free of porosity as determined with sectional metallography.

Results and Discussion

All welds made in this part of the study resulted in acceptable weld bead morphologies and a stable arc with a fixed weld parameter schedule. Remarkably, the welding was successful for all welding

Table 3 — Welding Parameter Schedule for Part 2

Welding Set Parameters	Set Voltage	Set Wire Feed Speed	CTWD (in.)	Travel Speed	Welding Time	Electrode Polarity
Part 1*	28 V	200 ~ 300 in./min (25 in./min step)	0.75	12 in./min	20 s	DCEN
Part 2	25 V	110 in./min	0.75	12 in./min	20 s	DCEN

*Welding parameters for Part 1 are shown for comparison.

wires with virtually no parametrical explorations by simply using the mid-range values suggested in a commercially available welding schedule published by the American Welding Society (Ref. 7).

Calorimetrically Measured Heat Input and Electrically Consumed Energy

Figure 1 shows the overall drop in measured heat input values of these Part 2 electrodes compared to one of the Part 1 electrodes, which is due primarily to the reduced wire feed rate setting and hence current used for all of the Part 2 study, but also reflects an approximately 25% reduction in total flux content. The lowered melting rate of the Part 2 study is believed to provide ample time for the self-regulation aspect of the welding process to occur to the fullest extent possible. The exothermic additions in the flux also have more time to react, and perhaps to a greater extent, within the arc, for the lower melting rate. The result is a reduction in electrode extension length that in turn leads to a longer, less efficient arc length for a fixed contact tube-to-work distance (CTWD).

The effect of average electrode extension lengths as a function of exothermic flux concentration for Part 2 electrodes are discussed later. The maximum heat input was observed at the 10 wt-% magnesium addition.

The electrical energy consumed must also be considered when looking at the effect of the exothermic additions on the calorimetrically measured heat input values. The electrical power consumed is plotted in Fig. 2. A minimum is recorded at the 20 wt-% level (ignoring the value of the 0 wt-% magnesium addition) that helps explain the minimum in measured heat input at that same level. The obvious maximum in electrical power consumed at the 10 wt-% concentration level corresponds to the maximum in measured heat input with calorimetry and confounds the ability to make simple heat input assessments directly for exothermic concentration levels. Recall that all Part 2 test welds were performed with identical welding parameters at a single melting rate. The variation in electrical power consumption is mainly the result of the electrical properties of the arc on the welding current. The

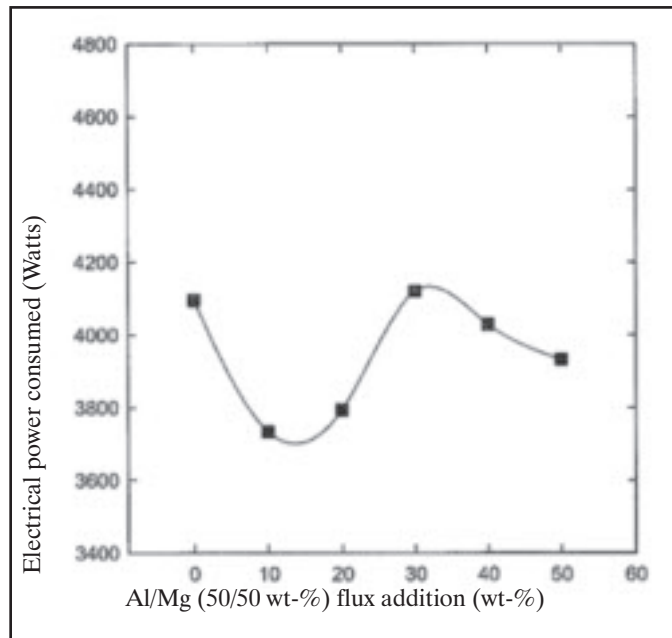
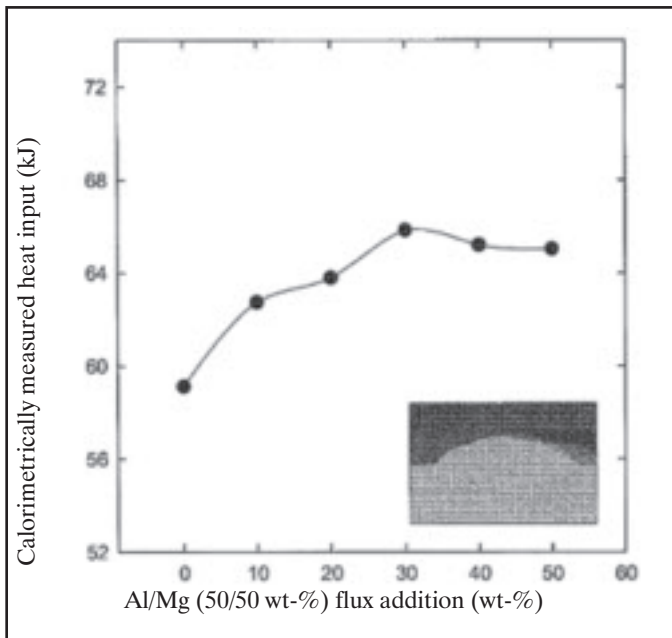


Fig. 5 — Measured heat input as a function of aluminum/magnesium (50/50 wt-%) flux addition at 110 in./min (47 mm/s) melting rate. The insert photography is bead morphology of weldment with 20 wt-% of Al/Mg (50/50) flux type electrode.

Fig. 6 — Electrical power consumed as a function of aluminum/magnesium (50/50 wt-%) flux addition at 110 in./min (47 mm/s) melting rate.

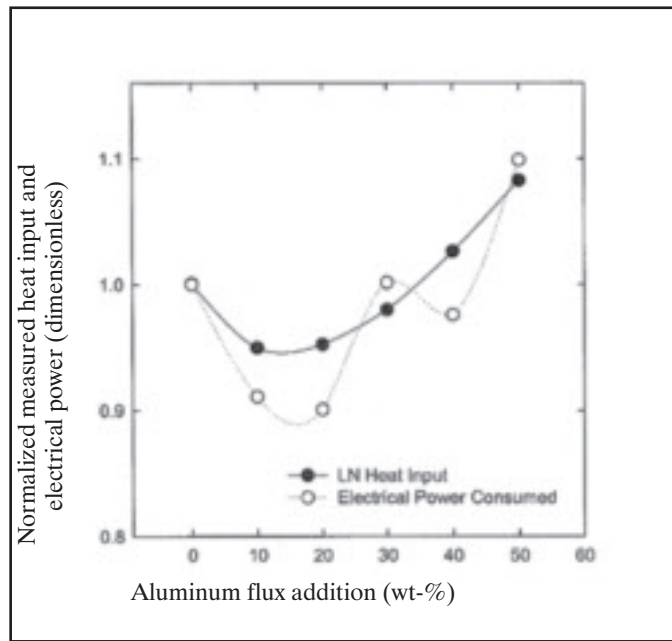
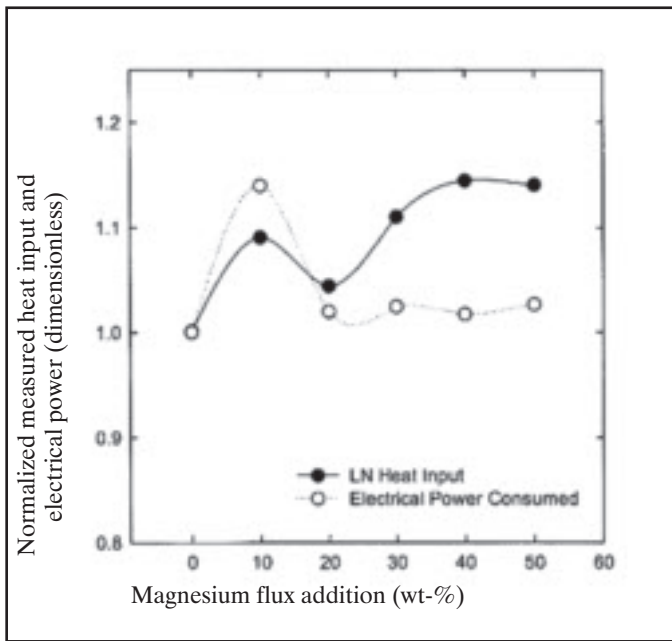


Fig. 7 — Normalized measured heat input and electrical power consumed as a function of magnesium flux addition at 110 in./min (47 mm/s) melting rate.

Fig. 8 — Normalized measured heat input and electrical power consumed as a function of aluminum flux addition at 110 in./min (47 mm/s) melting rate.

observed deviations between wires are ultimately due to the presence of the exothermic constituents introduced into the arc environment.

The measured heat input as a function of exothermic addition results for the aluminum-type flux are presented in Fig. 3. A minimum is recorded at the 30 wt-% level (below the 59 kJ posted for the 0 wt-%) aluminum addition electrode. Also, the measured heat input at 10 wt-% is below

that measured for the 20 wt-%. The 10 wt-% value and the 30 wt-% value measured less than that of the baseline, while the 20 wt-% value measured about the same. Beyond the 30 wt-% level the measured heat input appears to be linearly increasing. The gains in measured heat at the 40 and 50 wt-% value are likely due primarily to the increases in electrical power consumption measured at these concentration levels.

The power consumed in welding, as shown in Fig. 4, went way up with the 50 wt-% aluminum-type flux addition. These values were repeatedly measured. The measured heat input also correspondingly increased to a high value, although percentage-wise the increase was not nearly as extreme. The minimum power consumed occurs between the 10 and 20 wt-% flux levels and coincides with the minimum recorded in measured heat input.

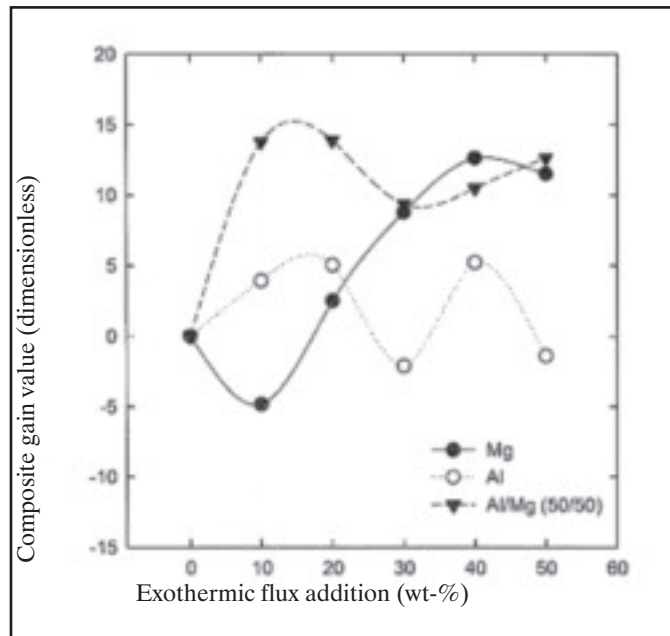
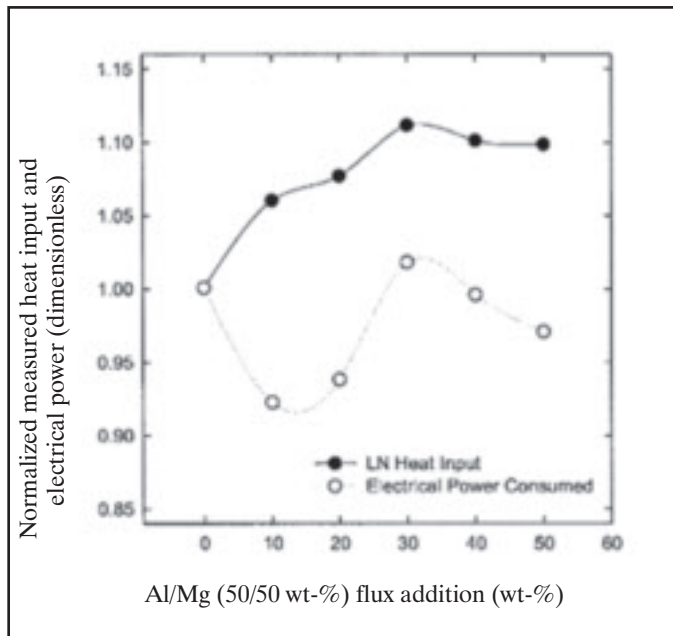


Fig. 9 — Normalized measured heat input and electrical power consumed as a function of Al/Mg (50/50 wt-%) flux addition at 110 in./min (47 mm/s) melting rate.

Fig. 10 — Net composite gain value or difference in normalized percentages between measured heat input and electrical power consumed as a function of exothermic flux addition.

For the fixed wire feed rate and voltage used, the consumed welding current is approximately proportional to the wire feed speed and should therefore be constant for these electrodes. Given the constant welding and setup parameters, any deviations in electrical power consumed must be due to a fundamental change in the electrical properties of the welding arc/electrode extension system brought on through the presence of the exothermic flux additions.

The measured heat input and electrical power consumed results for the Al/Mg (50/50 wt-%) type flux additions are presented in Figs. 5 and 6, respectively. All of the Al/Mg (50/50 wt-%) electrodes (Fig. 5) produced measured heat inputs greater than the 59 kJ posted for the baseline electrode. A maximum of 66 kJ, occurring at the 30 wt-% flux concentration, was recorded. The results appear much smoother through the concentration value range than for the singular aluminum- or magnesium-type flux addition cases. The arc behavior was subjectively smoother as well. The individual 20-s current and voltage traces for this type of electrode were uncharacteristically smooth and unvarying as compared with those of the other types of electrodes studied.

In the presence of both traditional types of exothermic additions, the burning of magnesium may make the ignition of the aluminum easier and/or more complete via catalytic reaction path kinetics within the welding arc of the FCA welding process. The lower combustion tempera-

ture of aluminum is, therefore, perhaps better suited for welding than the hotter-burning magnesium alone, while the presence of magnesium ensures more complete ignition and combustion of the aluminum. The presence of both types of metals in the welding arc may also enhance the electrical properties of the arc.

While the measured heat input as a function of exothermic concentration is smoothly increasing for the Al/Mg (50/50 wt-%) type flux, the electrical power consumed, as shown in Fig. 6, is not. A minimum of about 3700 W between the 10 and 20 wt-% concentration levels, below the 4100 W posted for the baseline weld, is exhibited. The apparent maximum of only 4115 W was observed at the 30 wt-% of Al/Mg (50/50) reactive addition, and this maximum was followed by exhibiting linearly decreasing electrical power with the 40 and 50 wt-% exothermic additions rather than increasing as with the other two (single exothermic component) flux types. The significant result here is that the measured heat inputs for the Al/Mg (50/50) type flux electrodes were strictly increasing from the baseline value with increasing concentration while the electrical power consumed dipped down below the baseline value. Then, the consumed power recovered to a mere 15 W above the baseline level (0.3% of the total average value) at 30 wt-% before dropping off again. The maximum measured heat input and the maximum electrical energy consumed points do coincide, however, at the 30 wt-% level for these Mg/Al-type flux-filled electrodes. Subjectively, all of the Al/Mg

(50/50) mix electrode types welded very smoothly. The arc was stable with only normal amounts of spatter, especially in the lower concentration levels.

Normalized Measured Heat Input and Electrically Consumed Energy

Dimensionless “normalized” heat input values are obtained by simply dividing out the heat input values, either calorimetrically measured or calculated from the electrical power, by those values taken from the baseline condition. Figure 7 depicts the normalized heat input and electrical power consumed as a function of wt-% magnesium-type flux addition. At the 10 wt-% level the large current draw, obviously, carries with it the large value for the measured heat input. The art of making sound welds in the spray mode with a continuous consumable electrode of experimental nature seemed to often result in unexpected electrical responses from the power supply. The real benefit, when corrected for the electrical energy consumed, appears to be around the 40 wt-% level. At the low wt-% of exothermic additions, it appears that the flux core has less ability to melt-back the electrode any additional amount than normal with the small amount of chemical heat available. Here the normal self-regulation current-voltage interaction is essentially unmitigated by the presence of such a small percentage of exothermic chemical addition.

The physical length of the electrode extension may not be so affected at low concentration levels as perhaps would be the

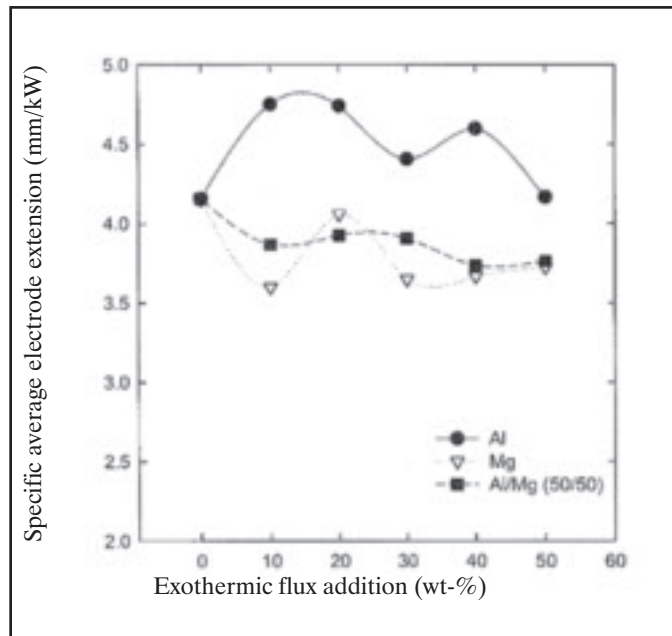
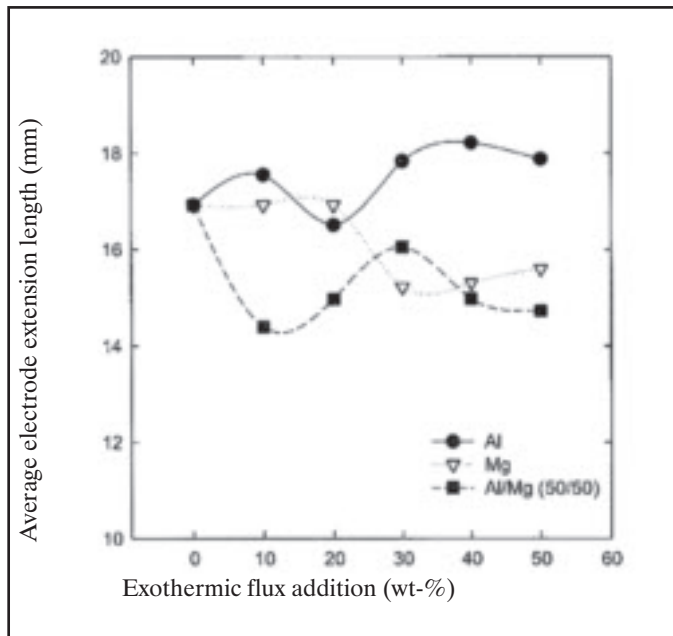


Fig. 11 — Average electrode extension length as a function of exothermic flux addition.

Fig. 12 — Average specific electrode extension length as a function of exothermic flux addition (specific electrode extension data are normalized values by the welding power from Fig. 11).

Table 4 — Percent Normalized Difference in Calorimetrically Measured and Heat Input from the Baseline Value

Wt-% Flux	10	20	30	40	50
Flux Addition Type					
Magnesium	9.1	4.4	11.1	14.4	14.1
Aluminum	-5.0	-4.8	-2.0	2.7	8.4
50-50 Al-Mg	6.0	7.7	11.2	10.1	9.8

Table 5 — Percent Normalized Difference in Electrical Power Consumed from the Baseline Value

Wt-% Flux	10	20	30	40	50
Flux Addition Type					
Magnesium	14.0	2.0	2.3	1.7	2.5
Aluminum	-9.0	-10.0	0.2	-2.6	9.8
50-50 Al-Mg	-7.8	-6.2	1.7	-0.5	-2.9

effects brought on through the electrical characteristics of the arc. A drop in arc resistance would cause a rise in current from the CP power supply for a constant power setting. At higher exothermic concentration levels, the shortening of the electrode extension dominates the electrical properties of the electrode extension/arc system. Both the aluminum and the 50/50 wt-% Al/Mg mix electrodes also display electrical extremes at the lowest concentration levels; however, the results are in the opposite direction from the magnesium-only case. Apparently, at the lower concentration levels the flux modification affects the current-carrying ability of the arc, whereas at the higher levels the electrode extension shortening dominates the electrical behavior of the electrode extension/arc couple.

Figure 8 shows the normalized heat input and electrical power consumed as a function of wt-% aluminum flux addition. It shows a minimum in normalized electrical power consumed and measured heat input at between the 10 and 20 wt-% ad-

dition levels. The effect is just the opposite observed with the magnesium flux filled electrode but perhaps to less extreme. It is speculated that the arc resistance is raised so that the current response from the CP power supply is negative. The normalized measured heat input from calorimetry is of course brought down by the electrical power minimization at the lower concentration levels. Again, at the higher levels of exothermic flux addition, the shortening of the electrode extension length maintains a dominant roll, and the measured heat input increases smoothly with the additional effects of chemical heating.

Figure 9 depicts the normalized heat input and electrical power consumed as a function of 50/50 wt-% Al/Mg-type flux addition. Results reveal the unexpected 8% rise in measured heat input opposite the 8% reduction in electrical power consumed in the area of 10 and 20 wt-% additions. The excess heat can only be explained by the generation of chemical heat. The other anomaly is the linear decrease in both the measured heat input

and the electrical power consumed at 30 wt-% and beyond. The slope in the reduction of measured heat input is less than the slope for the electrical power decrease. This indicates that chemical heating in the higher concentration levels is still significant and at the least measurable. The peak in measured heat input at the 30 wt-% level does, however, coincide with the peak in electrical power consumed. The additional current draw carries with it at this point a corresponding increase in measured heat input characteristic of welds performed without the benefit of exothermic chemical heat generation.

Composite Gain Values for Normalized Heat Input Benefit Plus Electrical Power Reduction

The benefits of utilizing exothermic flux additions appear through two mechanisms. The first is the creation of chemical heat directly via the intended chemical reactions while the other mechanism appears to be through a reduction in electrical energy consumed, as compared to the baseline condition. As with the electrodes of Part 1, a net composite gain value is calculated for the electrodes of Part 2. In the earlier study, decreases in normalized electrical power consumed with increases in wire feed speed (or melting rate) were recorded. This relationship is likely to hold for the Part 2 electrodes as well, although various melting rates were not investigated here. A reduction in arc resistance, brought on by the broadening influx of additional pure metal species of the

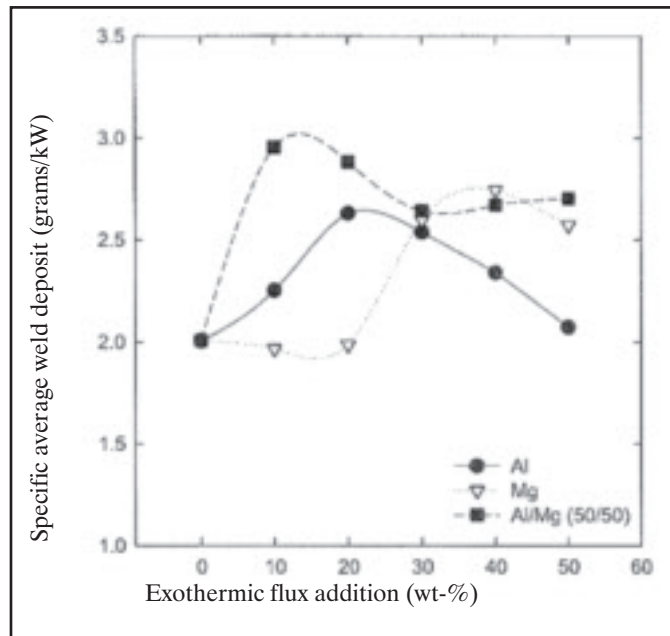
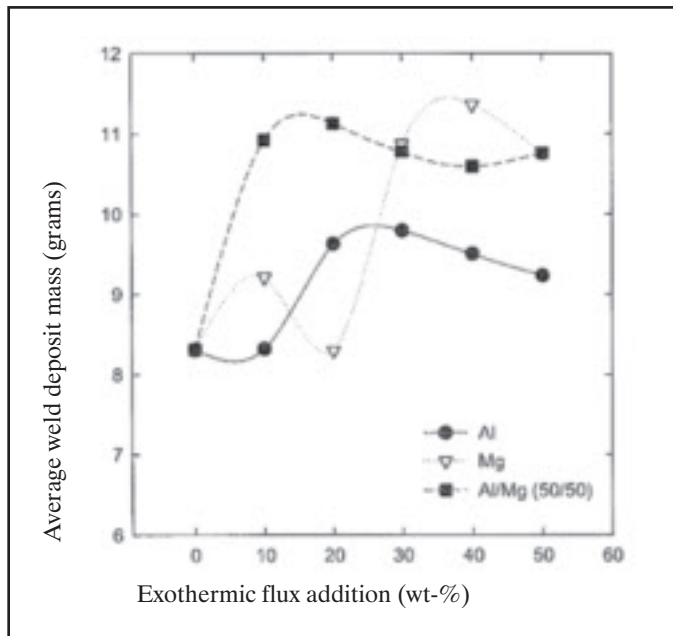


Fig. 13 — Average weld deposit mass as a function of exothermic flux addition.

Fig. 14 — Specific average weld deposit mass as a function of exothermic flux addition (specific weld deposit data are normalized values by the welding power from Fig. 13).

exothermic flux components (with lower resistivities compared to iron) and a shortening of the arc with increasing melting rate, could account for the apparent reduction in expected electrical power consumed. The normalized dimensionless parameter values are presented in tabular form. Table 4 lists the percent normalized difference from baseline in measured heat input of the Part 2 electrodes.

The highest increase in measured heat input occurs with the magnesium-type flux at 40 wt-% flux concentration. The value posted represents about a 14.5% increase over the baseline. The 50 wt-% magnesium-type electrode produced slightly less measured heat input at about 14% over the baseline. The apparent anomaly with the magnesium-type flux is at the 20 wt-% flux concentration level of only 4% above the measured heat input for the baseline. The 20 wt-% level is precisely the concentration level of the early magnesium-type flux that resulted in an overall experimental maximum of slightly more than a 22% increase from the Part 1 study. The Part 1 electrodes contain twice the magnesium as required by stoichiometry and were filled to 20% higher flux-to-sheath ratios. Also, the 200 in./min melting rate of the Part 1 electrode is just about twice the 110 in./min used in Part 2. These reasons may explain the differences in absolute measured heat values but do not explain the relative maximum/minimum difference.

The aluminum-type flux posted a maximum measured heat input at the 50 wt-% level of about 8% over the baseline. The -5% measured heat input at the 10 wt-%

was a minimum for all of the Part 2 electrodes. The trend of increasing relative measured heat input with aluminum-type flux addition is smoothly varying but when compared to the baseline value a minimum extreme occurs somewhere between the 10 and 20 wt-% levels and coincide with a large drop in electrical power consumed.

The percent normalized difference in calorimetrically measured heat input from the baseline value for the 50/50 wt-% Al/Mg-type flux shows a maximum of slightly more than 11% at the 30 wt-% concentration level. The minimum is recorded at the 10 wt-% level with a 6% increase in measured heat over the baseline. The smooth all positive responses of the 50/50 wt-% Al/Mg electrode and the smooth largely negative responses of the aluminum-type electrode contrast with the extremes of the magnesium-type electrode.

The percent normalized difference in electrical power consumed from the baseline condition is presented in Table 5. The noticeable result is the obvious spike in relative electrical power consumed of the magnesium-type electrode at the lowest wt-% tested. Magnesium, like aluminum, has a higher electrical conductivity value than iron, and like aluminum, the oxide formed via the exothermic reaction leads to a rather effective electrical insulator. When introduced in powdered form into the arc environment at the expense of the iron, one might expect that the arc resistance should either be raised or lowered compared to the baseline condition. An interesting fact concerning power transfer through a variable load resistor is that the

power absorbed by this resistor is maximized when the load resistance happens to equal the instantaneous internal power source resistance (see Appendix). Also, power cannot be absorbed whenever the load resistance is infinite (open circuit) or zero (short circuit), and all of the energy absorbed by the load resistor is dissipated and converted to heat by the resistor. Practically no other "work" is being performed by this energy. The point is that whenever the load resistance, in this case the arc resistance, passes through an ohmic value precisely equal to the internal resistance of the CP power supply, then the power dissipated and converted to heat in this load resistor will pass through a maximum. Perhaps the combination of easily ionized, highly conductive pure metal powders and the rapid creation of metal oxides of negligible electrical conductivity within the arc are modifying the arc resistance such that a peak in power consumed occurs. If this situation is indeed the case, then one could calculate the arc/electrode extension resistance at this point knowing the source voltage and source resistance values. The source resistance could be modulated for a given welding condition until the power consumed, as measured by the welding current, was maximized. That this measured peak in relative power consumed for the magnesium-type electrode is, in fact, the maximum recorded throughout this study lends credence to the idea of a resonant arc (load) resistance value being encountered.

The arc resistance can never be negative and as such the electrical power con-

Table 6 — Net Composite Gain Value (Dimensionless Normalized Energy Scalar)

Wt-% Flux	10	20	30	40	50
Flux Addition Type					
Magnesium	-4.9	2.5	8.8	12.7	11.5
Aluminum	3.9	5.1	-2.2	5.3	-1.5
50-50 Al-Mg	13.8	13.9	9.5	10.7	12.8

sumed cannot be negative, but the difference in normalized electrical power consumed compared to the baseline value can be, as is the case for the aluminum and 50/50 wt-% Al/Mg type electrodes. The 50 wt-% aluminum-type flux electrode shows a high value for relative power consumed, similar to but slightly less than the maximum recorded for the 10 wt-% magnesium electrode. It is speculated that the arc resistance here is also approaching that of the power supply, resulting in a relative peak in power consumed. It does not matter from which side of this supply resistance value that the arc (load) resistance approaches, only that a maximum power transfer condition results when they are equal and a relative local maximum is encountered when the absolute difference is minimal.

The net composite gain values are tabulated in Table 6 and plotted in Fig. 10. The maximum net composite gain value occurs between the 10 and 20 wt-% electrodes of the 50/50 wt-% Al/Mg type flux. These electrodes used much less electrical power than the baseline comparative while posting positive gains in relative measured heat input values. With both aluminum and magnesium metal powder additions, each with a lower electrical resistivity value than iron, the electrical resistance of the electrode extension is likely less than that of the pure iron powder baseline. With more than one possible reaction path available over a large temperature range within the arc, the resulting kinetics is perhaps most favorable with this type of flux as well. The arc is known to have regions of constant temperature, both spatially within the arc volume and quantitatively over a wide range of current values. Some regions may favor the reactions that associate themselves with the "best" temperature of combustion in the cooler outermost regions of the arc and near the boundary layers surrounding the superheated molten droplets. These "mixed" type electrodes were subjectively the smoothest welding electrodes of the combined studies.

The next-highest net composite gain value occurs with the 40 wt-% magnesium-type electrode. At this concentration level,

Table 7 — Average Welding Electrical Consumption Values, Electrode Extension Lengths, and Specific Deposit Masses for Part 2 Electrodes

Electrode Type	Avg. Voltage (V)	Avg. Current (A)	Avg. Power (kW)	Avg. Electrode Extension (mm)	Specific Electrode Extension (mm/kW)	Avg. Deposit (g)	Specific Deposit (g/kW)
Baseline	26.1	154.9	4.05	16.9	4.2	8.1	2.0
Al flux additions							
10% Al	26.2	140.4	3.7	17.5	4.8	8.3	2.3
20% Al	26.0	133.8	3.5	16.5	4.8	9.3	2.6
30% Al	26.1	155.0	4.1	17.8	4.4	10.3	2.5
40% Al	26.2	150.2	4.0	18.2	4.6	9.3	2.2
50% Al	26.3	162.5	4.3	17.8	4.2	8.9	2.1
Group Avg.	26.2	148.2	3.9	17.5	4.5	9.2	2.2
Mg flux additions							
10% Mg	26.3	177.6	4.7	16.8	3.6	9.2	2.0
20% Mg	26.2	159.1	4.2	16.8	4.0	8.3	2.0
30% Mg	26.3	159.6	4.2	16.8	3.6	10.8	2.6
40% Mg	26.2	158.9	4.2	15.2	3.7	11.4	2.7
50% Mg	26.2	160.0	4.2	15.2	3.7	10.8	2.6
Group Avg.	26.2	163.0	4.3	15.9	3.7	10.1	2.4
Al/Mg (50/50) flux additions							
10% Al-Mg	26.0	143.8	3.7	14.5	3.9	11.1	3.0
20% Al-Mg	26.1	145.3	3.8	15.0	3.9	11.0	2.9
30% Al-Mg	26.2	157.0	4.1	16.1	3.9	10.1	2.7
40% Al-Mg	26.2	153.8	4.0	15.1	3.8	10.8	2.7
50% Al-Mg	26.1	150.3	4.0	14.7	3.8	10.6	2.7
Group Avg.	26.1	150.0	4.0	15.1	3.8	10.9	2.8

this type of electrode posted the highest normalized measured heat input (Table 6) in spite of the large spike in electrical power consumption at the 10 wt-% level.

The aluminum-type electrode shows two peaks in net composite gain value of about 5% occurring at the 20 and 40 wt-% levels. In between, at the 30 wt-% level, a spike in relative electrical power consumed (as shown in Fig. 4) happens to occur. The dip might be due to a resonant arc/electrode extension resistance value being encountered, and when the equivalent electrical heat is subtracted from the measured heat value, a local dip between the bordering net value results.

Electrode Extension Lengths and Weld Deposit Mass

When considering the arc as a variable load resistor in a simple circuit, the property of electrical conductivity or the inverse, electrical resistivity, of the changing components of the arc/electrode extension system (namely the exothermic flux additions) must be considered. The exothermic flux additions are the only constituents being systematically changed that can alter the properties of the arc/electrode extension environment. Table 7 lists the average voltages, current,

electrical power consumed, and average measured electrode extension lengths along with average deposit mass and normalized (specific) electrode extension and deposit masses.

Although the set machine voltage for all welds was 25 V, the measured results were consistently 26 V. The higher voltage realized may be due to a shorter average electrode extension length than normally achieved with commercial FCA welding electrodes, a result of the exothermic additions, even for the baseline. Figure 11 shows the average electrode extension lengths as a function of exothermic flux concentration. Very little variation is noted. At the 30 wt-% and above level, the aluminum-type electrode extension is about 2 mm longer than the magnesium and 50/50 wt-% type electrodes and only about 1 mm longer than the baseline. Figure 12 shows the electrode extension data normalized by the welding power. In this case all of the aluminum-type electrodes have longer normalized electrode extension lengths than the baseline electrode while all of the magnesium and 50/50 wt-% type electrodes have shorter lengths.

Aluminum has a lower resistivity than the magnesium so the resulting joule heating of the electrode extension might be less for this type of electrode. At the time

that this research was conducted in the late 1990s, all of the available GMA welding electrode extension computer models reported a predicted length to no better than plus and minus the electrode diameter. For the 1/16-in.-diameter electrodes used for this research that error equates to about 1.6 mm. The “shut off and snip” method employed appears valid to the same tolerance level or better if the diameter of the ball forming at the end, if present, or any hint of the formation of the ball is ignored. While the measurements and the accounting data are recorded to one or two decimal places, this practice was carried out in an effort to maintain precision for comparative purposes internal to this study and is, obviously, not meant to imply such a high level of absolute accuracy. Room-temperature measurements with a digital ohm meter of the welding machine apparatus taken from a representative electrode tip and work surface (with the system shut down) were inconclusive suffice to say that it was less than 500 mΩ. The suspected arc load resistance variation and its effect on the power consumption through the power supply along with the self-regulation aspect on electrode extension length precludes direct assessment of exothermic flux additions on electrode extension length at this time.

The average weld deposit mass as a function of exothermic flux addition concentration level is given in Fig. 13. All of the electrodes recorded deposit masses greater than the baseline electrode except for the 10 wt-% aluminum and 20 wt-% magnesium type flux electrodes, which at least matched the baseline deposit mass. The highest deposit values were recorded with the 10 and 20 wt-% reactive additions in 50/50 wt-% Al/Mg flux type electrodes at around 11 g. The 40 wt-% magnesium flux type recorded the maximum deposit mass of 11.35 g. The 30 wt-% aluminum type flux electrode recorded a group maximum of 10.3 g. Not surprisingly, maximum deposit values of this group coincide with overall arc process efficiency maxima in 50/50 wt-% Al/Mg flux. Worth noting, however, is the fact that small adjustments to the welding parameter schedule might well optimize any specific Part 2 electrode. Higher melting rates, for instance, would likely result in higher exothermic heat benefits along with higher deposit masses.

Figure 14 shows the average weld deposit mass normalized by the welding power consumed as a function of wt-% exothermic flux addition. The results clearly show the benefits of the exothermic additions in average mass of weld deposit per kW electrical energy consumed. The 10 wt-% of Al/Mg flux type electrode recorded a specific deposit of 3 g deposit

per kW consumed. The result represents a 50% increase over the 2 g/kW of the baseline average. Second highest of all the electrodes in specific deposit occurred with the 40 wt-% magnesium flux type electrode with 2.7 g/kW, a 35% increase. The highest specific deposit for the aluminum flux type group occurred at the 20 wt-% level with a 2.6 g/kW value, a 30% increase from the baseline value. None of the Part 2 electrodes underperformed the baseline in specific weld deposit results. A 50% increase in specific deposit with only a 10 wt-% modification to a commercial self-shielded FCA welding flux formula using “canned” welding parameters and achieving a sound weld is rather remarkable. One could conceivably save half in electrical energy or weld 50% more with the same electricity. Further gains are likely feasible with parametric electrode optimization studies.

Conclusions

Based on the experimental results obtained in this study, the following conclusions were summarized:

1. The highest increase in normalized measured heat input for this Part 2 study over the new baseline electrode occurs with the magnesium-type flux at a 40 wt-% flux concentration of 14% over the baseline.
2. The aluminum-type flux posted a maximum measured heat input at the 50 wt-% level of about 8% over the baseline.
3. The calorimetrically measured heat input from the baseline value for the Al/Mg (50/50) type flux shows a maximum of slightly more than 11% at the 30 wt-% concentration level.
4. The maximum net composite gain value occurs between the 10 and 20 wt-% electrodes of the wt-% Al/Mg (50/50) type flux. These electrodes used much less electrical power than the baseline comparative while posting positive gains in relative measured heat input values.
5. All of the aluminum-type electrodes have longer normalized electrode extension lengths than the baseline electrode while all of the magnesium and Al/Mg (50/50) electrodes have shorter lengths.
6. All of the electrodes recorded deposit masses greater than the baseline electrode. The highest deposit values were recorded with the 10 and 20 wt-% Al/Mg flux type electrodes.

Acknowledgments

The authors acknowledge and appreciate the support of the U.S. Army Research Office, Savannah River National Laboratory, and Dong-Eui University.

Appendix: Maximum Electrical Power Transfer* or One Reason Why Arc Welding Processes Show Variance

BY S. H. MALENE

Enough is presently known about the gas tungsten arc welding (GTAW) process to be able to calculate the energy needed to obtain a desired depth of penetration in a given type of metal. However, the arc process efficiency values can range from 0 to 95% efficient for the process in general, and can easily run to $\pm 10\%$ within a “qualified” welding process. Therefore, there is as yet no substitute for running qualification welding runs. The electronic controls are very precise but the nature of the arc plasma itself is the primary cause of much of the imprecision. The interrelationships of the primary process variables can act to exacerbate this imprecision, or with proper development and statistically derived nominal settings, much of the vagary can be effectively damped out. This later situation leads to a “robust” welding process that is generally very repeatable. However, on occasion even a well-developed arc welding process can “go away” and may need to be “redeveloped.” Very subtle changes within the arc environment can interact with the welding power supply resulting in unpredicted outcomes of the physical properties of the weld. Not enough is known about the physics of the plasma to be able to control or measure the necessary physical characteristics to effect closer tolerance of the process. Similar conditions exist with resistance welding, only substitute “the volume of metal undergoing joule heating and plastic deformation” for the arc plasma and “resistance welding” for GTAW in the following descriptions. The following discussion utilizes Ohm’s law to elucidate one probable

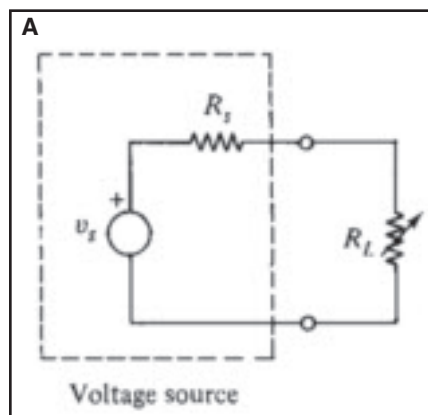


Fig. A — Simple circuit. R_L = variable load resistor; R_S = “fixed” welding system resistance between the arc anode and cathode; and V_S = the welding supply voltage.

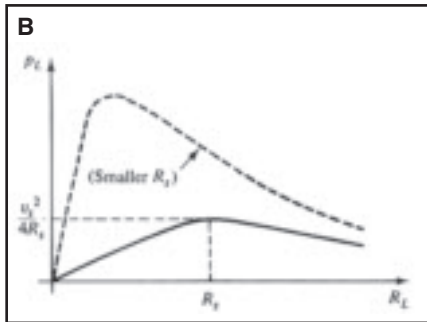


Fig. B — Graphical representation of P_L , the power dissipated in the arc, as a function of R_L , the variable arc load resistance.

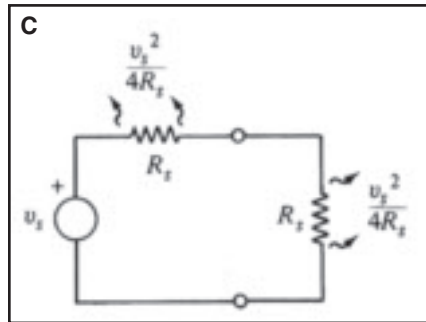


Fig. C — Simple circuit schematic representation of the maximum power dissipation condition. $R_L = R_S =$ one-quarter of the square of the supply voltage divided by this resistance.

cause for GTAW weld variability. The outcome of the discussion is meant to show that at least one source of this variability, a change in the internal power supply resistance, can be minimized by using identical welding machine equipment and ancillary process setup items for both development and production.

Consider the welding arc as the variable load resistor R_L in the simple circuit of Fig. A. R_S is the “fixed” welding system resistance between the arc anode and cathode, V_S is the welding supply voltage. For a resistor, the terminal variables are related through Ohm’s law, $V = IR$, so that the power delivered into the load resistor is as follows: $P = VI = I^2R = V^2/R$.

Since either the voltage V or the current I is squared in the power relationship, the power delivered into a resistor R cannot be negative. A resistor always resists current flow and therefore will always absorb power. The energy absorbed by the load resistor is the power (as a function of time) integrated over time, given in watts (as a function of time), $W(t)$:

$$W(t) = \int_0^t P(t') dt' = R \int_0^t I^2(t') dt'$$

$$= \frac{1}{R} \int_0^t V^2(t') dt'$$

All of the energy absorbed by the load resistor R_L is dissipated physically by the resistor in the form of heat. All of the power (P_S of the R_S , V_S combination in the dashed box of Fig. A) supplied by the voltage V_S goes into the load resistor R_L . Therefore, the power P_L , dissipated in the welding arc is the power received by the arc in load resistance R_L :

$$P_L = I^2 R_L = \left(\frac{V_S}{R_S + R_L} \right)^2 R_L$$

When the arc resistance is zero, representing an electrode stub-out condition, or infinite, representing the open circuit condition, no power is delivered by the supply and no heat is generated. Stated succinctly, a short or open circuit cannot transfer any power.

Obviously from the latest equation for the power absorbed by the load, P_L above, for some value of R_L between infinity and zero the power absorbed will peak. To find the value of R_L that will maximize the load power, P_L is differentiated with respect to R_L , the result is then set to zero and solved for R_L :

$$\frac{dP_L}{dR_L} = \frac{V_S^2 \left[(R_S + R_L)^2 - 2R_L(R_S + R_L) \right]}{(R_S + R_L)^4}$$

$$= V_S^2 \frac{(R_S + R_L)}{(R_S + R_L)^3} = 0$$

This is true whenever $R_L = R_S$. Thus, when the arc resistance precisely matches the resistance of the voltage source (the resistance of the combined welding power supply, workpiece, electrode, and leads), the maximum power available is supplied to the arc. By substituting the now equivalent resistance values into the expression for the power of the arc (load), the maximum power dissipated by the arc becomes:

$$(P_L)_{MAX} = \left(\frac{V_S}{R_S + R_L} \right)^2 R_L \Big|_{R_L=R_S} = \frac{V_S^2}{4R_S}$$

To control the performance of a welding power supply, the operator sets the voltage value or the current level, and the supply manufacturer minimizes the internal resistance. Interestingly, the power being dissipated in the arc, P_L , during welding is also being matched and dissipated by that of the power supply, P_S . The same quantity of heat energy being used to

weld from the arc is being dissipated by the power supply. A welding power supply of finite size must therefore periodically be allowed to idle a certain percentage of the time used for welding to avoid a meltdown of the internals. Manufacturers express this in terms of a machine duty cycle for a given power setting. Duty cycle is the amount of idle time to welding arc-on time in a 10-min interval for a given power setting in percent. In general, of course, the load resistance is semifixed in the steady-state welding condition while the power supply and the weld fixturing fix the source (internal) resistance. The power supply usually gives less power than it is capable of, the maximum allowed by the machine settings, except whenever the arc resistance happens to match the supply resistance.

Figure B is a graphical representation of the power dissipated in the arc, P_L , as a function of the variable arc load resistance R_L . Minimization of the internal power supply resistance by using massive copper windings provides for the highest available power and allows for good heat dissipation and higher duty cycles, but at higher material costs.

The dashed line represents a smaller internal supply resistance, by a factor of three, from the solid line resistance, and can therefore result in three times the maximum available power.

Figure C is a simple circuit schematic representation of the maximum power dissipation condition, when $R_L = R_S =$ one-quarter of the square of the supply voltage divided by this resistance. The power that must be physically dissipated in the form of heat for both resistors, the arc and the power supply, is the same maximum value. Of course the welding arc is not just a simple variable load resistor but has capacitance and inductance properties as well, and the heat dissipated (produced for welding) is not all due to joule (I^2R) heating.

The gas tungsten arc welding process utilizes a constant-current type of power supply. For a given cover gas the voltage is a direct linear function of the physical arc gap dimension, the distance from the work surface to the tungsten electrode surface (the distance between the anode and cathode terminal ends defining the arc length) barring surface charge effects. Any physical change in this dimension during welding changes the voltage and therefore, for a given current setting, the arc resistance. If this change is toward the “peak” value, coming from either side, the actual power delivered into the work will change to a higher value. Likewise, if the arc resistance changes away from the peak value a lesser amount of power will be supplied. Anything that affects the instantaneous

resistance value of the arc column will have an effect on power consumption.

Commercial power supplies are made to operate in the most efficient region — that necessarily being close to that yielding maximum power for a given operating range. Therefore, small perturbations from either within the arc environment or changes to the internal resistance of the machine and ancillary components can easily result in measurable variations in heat input that will physically relate to weld geometry variations. Usually the depth of penetration is the primary response variable to changes in heat input. Clearly, small variations in welding machine and ancillary equipment internal resistance values can have a significant effect on the outcome of a welding operation. Differences between machine manufacture brands and models are expected.

Also of note is that Ohm's law cannot hold within the arc when the charge carrier species are physically changing in type and amount as might be expected to result

from nonsteady-state transient power consumption variations. The maximum power transferred from a welding machine through the arc will occur whenever the arc load resistance matches the system hardware internal resistance in a resonant (value over time) manner. This phenomenon is offered here as a partial explanation for the apparent dependence of arc welding processes on the operator and development engineer skill level and expertise. A simple technique to minimize this dependence is to use identical welding equipment through development and into production.

**Budak, A. 1987. Circuit Theory Fundamentals and Applications, 2nd ed. Englewood Cliffs, N.J.: Prentice-Hall, Inc., ISBN 0-13-134057-3 025, pp. 136-140.*

References

1. Allen, J. W. 1994. Exothermically assisted shielded metal arc welding. MS thesis # T-4629, Colorado School of Mines, Golden, Colo.

2. Allen, J. W., Olson, D. L., and Frost, R. H. 1998. Exothermically assisted shielded metal arc welding. *Welding Journal* 68(7): 277-s to 285-s.

3. Malene, S. H., Park, Y. D., and Olson, D. L. 2007. Response of exothermic additions to the flux cored arc welding electrode — Part I. *Welding Journal* 86(10): 293-s to 302-s.

4. Glushchenko, A. S. 1980. Determination of the productivity of the thermit arc welding process under an exothermic flux. *Svar. Proiz.* No. 9: 25-27.

5. Karpenko, V. M. 1980. The melting parameters of welding electrodes with an exothermic coating mixture. *Svar. Proiz.*: 33-37.

6. Glushchenko, A. S. 1980. Determination of the productivity of the thermit arc welding process under an exothermic flux. *Svar. Proiz.*: 37-39.

7. The American Welding Society. 1995. *Standard Welding Procedure Specification (WPS) for Self-Shielded Flux Cored Arc Welding of Carbon Steel*, ANSI/AWS B2.1-1-027-95, p. 3, Miami, Fla.

Statement of Ownership, Management and Circulation for U.S. Postal Service (Required by U.S.C. 3685)

- | | |
|---|---|
| 1. TITLE OF PUBLICATION: Welding Journal
3. DATE OF FILING: September 29, 2007
5. NO. OF ISSUES PUBLISHED ANNUALLY: 12
7. MAILING ADDRESS OF KNOWN OFFICE OF PUBLICATION: 550 N.W. LeJeune Rd., Miami, Dade County, Florida 33126
8. MAILING ADDRESS OF THE HEADQUARTERS OR GENERAL BUSINESS OFFICES OF THE PUBLISHERS:
550 NW LeJeune Rd., Miami, Dade County, Florida 33126
9. NAMES AND COMPLETE ADDRESS OF PUBLISHER, EDITOR AND MANAGING EDITOR:
PUBLISHER: Andrew Cullison, AWS, 550 NW LeJeune Rd., Miami, Florida 33126
EDITOR: Andrew Cullison, AWS, 550 NW LeJeune Rd., Miami, Florida 33126
MANAGING EDITOR: Zaida Chavez
10. OWNER: NAME: American Welding Society, Inc. ADDRESS: 550 NW LeJeune Rd., Miami, Florida 33126
11. KNOWN BONDHOLDERS, MORTGAGEES, AND OTHER SECURITY HOLDERS OWNING OR HOLDING 1 PERCENT OR MORE OF TOTAL AMOUNT OF BONDS, MORTGAGES OR OTHER SECURITIES: None
12. The purpose, function, and nonprofit status of this organization and the exempt status for Federal income tax purposes:
Has not changed during preceding 12 months
13. Publication Title: Welding Journal
15. EXTENT AND NATURE OF CIRCULATION: | 2. PUBLICATION NO.: ISSN 0043-2296
4. FREQUENCY OF ISSUE: Monthly
6. ANNUAL SUBSCRIPTION: \$120.00
14. Issue date for Circulation Data Below: October 2007 |
|---|---|

	Average No. Copies Each Issue During Preceding 12 Months	Actual No. Copies of Single Issue Published Nearest to Filing Date
A. Total No. Copies Printed (Net Press Run)	53,250	54,200
B. Paid and/or Requested Circulation		
1. Paid / Requested Outside-County Mail Subscriptions Stated on Form 3541	51,316	52,471
2. Paid In-County Subscriptions Stated on Form 3541	None	None
3. Sales Through Dealers and Carriers, Street Vendor, Counter Sales, and other Non-USPS Paid Distribution	None	None
4. Other Classes Mailed Through the USPS	None	None
C. Total Paid / Requested Circulation	51,316	52,471
D. Free Distribution by Mail (Samples, complimentary and other free)		
1. Outside-County as Stated on Form 3541	402	414
2. In-County as Stated on Form 3541	None	None
3. Other Classes Mailed Through the USPS	None	None
4. Free Distribution Outside the Mail (Carriers or other means)	None	None
E. Total Free Distribution	402	414
F. Total Distribution	51,718	52,885
G. Copies not Distributed	1,532	1,315
H. Total	53,250	54,200
I. Percent Paid and / or Requested Circulation	99.2%	99.2%

16. Statement of Ownership will be printed in the November 2007 issue of this publication.
 I certify that the statements made by above are correct and complete:
 Andrew Cullison, Publisher